Supplementary Information (SI) for Journal of Materials Chemistry C.

Supporting Information

Synergistic Effects of Triplet-Triplet Annihilation and Reverse Intersystem Crossing in a Platinum-Based Electrochemiluminescent Metallopolymer Emitter

Chun Hong Mak[a,b], Yaojia Ai[e], Chunyan Tan[d], Wenxin Niu, Kuan-Chen Cheng, Chang-Wei Hsieh, Hsin-Hui Shen, Zheng Hu, Yanqing Tian, Xue-Qing Xu, Guizheng Zou[e,*], Duu-Jong Lee[b,*], Hsien-Yi Hsu[a,c,f,*]

[a] School of Energy and Environment, City University of Hong Kong, Kowloon Tong, Hong Kong, China.

[b] Department of Mechanical Engineering, City University of Hong Kong, Kowloon Tong, Hong Kong, China

[c] Department of Materials Science and Engineering, Centre for Functional Photonics (CFP), City University of Hong Kong, Kowloon Tong, Hong Kong, China.

[d] The State Key Laboratory of Chemical Oncogenomics, the Graduate School at Shenzhen, Tsinghua University, Shenzhen 518055, P. R. China.

[e] School of Chemistry and Chemical Engineering, Shandong University, Jinan 250100, China.

[f] Shenzhen Research Institute of City University of Hong Kong, Shenzhen 518057, P. R. China

Contents

Part A Experimental details S2-S4

Part B Synthesis details

Scheme S1 Synthetic procedure S5-S8

Part C NMR spectrum

Figure S1 ^{1}H NMR spectrum of TIPS-BTD-TMS S9
Figure S2 ^{13}C NMR spectrum of TIPS-BTD-TMS S9
Figure S3 ^{1}H NMR spectrum of TIPS-BTD. S10
Figure S4 ^{13}C NMR spectrum of TIPS-BTD. S10
Figure S5 ^{1}H NMR spectrum of TIPS-BTD-Pt. S11
Figure S6 ^{13}C NMR spectrum of TIPS-BTD-Pt. S11
Figure S7 ^{1}H NMR spectrum of BTD-Pt. S12
Figure S8 ^{13}C NMR spectrum of BTD-Pt. S12
Figure S9 ^{1}H NMR spectrum of p-PtBTD. S13

Part D Supporting Data

Figure S10 Transient PL decay of p-PtBTD S14
Figure S11 TAS kinetic trace of p-PtBTD probed at 690 nm and 514 nm S14
Figure S12 Tafel plot of the 1st reduction peak, 2nd reduction peak, and oxidation peak of p-PtBTD S14
Figure S13 Enlarged ECL spectrum of 1 mM p-PtBTD pulsed in DCM S17
Figure S14 ECL intensity of Rubpy$_3$ and p-PtBTD under concentration of TPrA experimental conditions S17
Table S1 Kinetics of p-PtBTD monitored at 584 nm at different temperatures. S18

Table S2 ECL efficiencies of Rubpy$_3$ and p-PtBTD under different concentration of TPrA. S18

A. Experimental details

Ultrapure fresh water was obtained from a Millipore water purification system (>18MΩ Milli-Q, Millipore). Anhydrous acetonitrile (MeCN), Anhydrous dichloromethane (CH_2Cl_2 or DCM) and tripropylamine (TPrA, 98%) were obtained from Aldrich and transferred directly into a argon atmosphere glovebox (Vacuum Technology Inc., Gloucester, MA, USA) without further purification. Electrochemical-grade tetra-n-butylammonium hexafluorophosphate ($TBAPF_6$), 2,5-dibromothiophene, tri-isopropylsilylacetylene and trimethylsilylacetylene were obtained from Alfa Aesar and used as received. All the reactions were prepared under N_2 atmosphere in the glovebox (< 0.1 ppm H_2O, < 0.1 ppm O_2). All syntheses were performed under argon atmosphere in anhydrous solvents, which were dried prior to use following standard procedures. Merck silica gel 60 (particle size 0.04−0.063 mm) was employed for flash chromatography.

Characterization

For UV−visible absorption measurements, samples were dissolved in DCM and were carried out on a LAMBDA 1050+ UV/Vis/NIR spectrophotometers (PerkinElmer Inc., USA) using 1 cm path length sealed quartz cells. Photoluminescence measurements were obtained with 360 nm excitation on a RF-5301PC (Shimadzu Scientific Instrument) using 1 cm square sealed quartz cells. Time-resolved PL measurements were made using a time correlated single photon counting setup (PicoQuant GmBH). The temperature-dependent experiments used cryostat (OptistatDN-X, Oxford Instrument, UK) to control the temperature of the samples. Samples were photoexcited using a laser head providing < 200 ps pulses with a fluence of ~ 30 nJ cm^{-2}. ^1H nuclear magnetic resonance (NMR) spectra were recorded with a Bruker AVANCE 300 instrument using deuterated chloroform ($CDCl_3$) as the solvent. High-resolution mass spectrometry was performed on a Bruker APEX II 4.7 T Fourier transform ion cyclotron resonance mass spectrometer (Bruker Daltonics, Billerica, MA). Ultrafast pump-probe experiments were performed with femtosecond (fs) transient absorption spectroscopy (Ultrafast System, Helios, USA). The pump pulses at 360 nm were created from fs pulses generated in an optical parametric amplifier (Newport Spectra-Physics). The sample solution in the sealed cell was constantly stirred to avoid photodegradation in scanned volume. The pump and probe beams were overlapped both spatially and temporally on the sample solution, and the transmitted probe light from the samples was collected on the broad-band UV-visible-near-IR detectors to record the time-resolved excitation-induced difference spectra.

Electrochemistry

For cyclic voltammogram (CV) and electrochemiluminescence (ECL) experiments, the three-electrode conventional electrochemical cell consisted of a Pt wire (1 mm in diameter) as a counter electrode, a Ag/AgNO$_3$ as a reference electrode, and a Pt disk (2 mm in diameter) inlaid in PTFE act as a working electrode. The geometric area of the Pt disk electrode was 0.0314 cm^2. After each experiment, the potential of the Ag/AgNO$_3$ reference electrode was calibrated with ferrocene as internal standard (0.201 V vs SCE).[1] The working electrode was polished with alumina particles and cleaned by sonication in Milli-Q deionized water and then in ethanol before the experiment. The clean-up procedures of counter and reference electrodes were processed by sonicating in acetone, water, and ethanol, finally were rinsed with D.I. water, dried in ambient condition and then transferred into a glovebox.

All solutions for electrochemical measurements consisted of 1 mM p-PtBTD in DCM as the solvent with 0.1 M TBAPF$_6$ as the supporting electrolyte. For the measurement under ambient condition, the electrochemical cell and ECL cell with sample solution were protected with airtight sealed teflon cap to avoid any O$_2$ contamination. To connect with the electrode inside the electrochemical cell, the stainless-steel rods as a conductor were driven through the cap. CV were obtained on a CHI 760E CH Instruments electrochemical workstation (Chenhua Co., Shanghai, China)

Electrochemiluminescence (ECL)

The ECL spectra were obtained on homemade system coupling a PyLoN charge-coupled device (CCD) camera (Teledyne, USA) cooled to –100°C with an Acton SpectraPro 2300 monochromator (Acton, MA) as the detector. CV-ECL plots and ECL intensity - time plots were collected on an MPI-E ECL analyzer (Xi'an Remax Analyse Instrument Co., Ltd., Xi'an, China). The PMT was supplied with −800 V.

B. Synthesis Details:

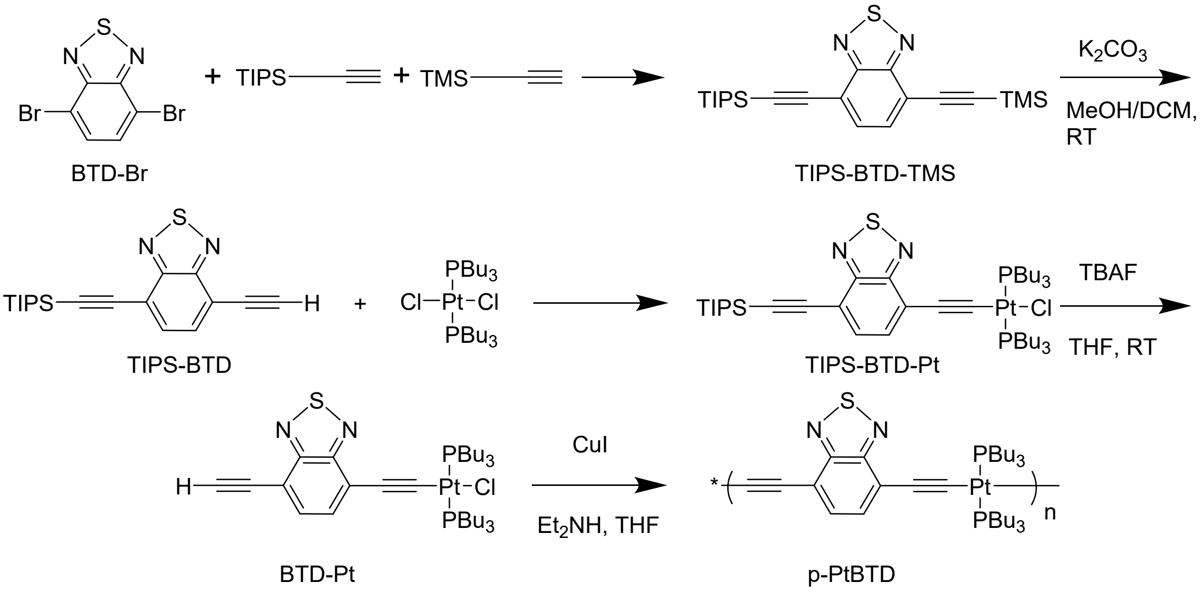

Scheme S1. Synthetic procedure of p-PtBTD.

4-((triisopropylsilyl)ethynyl)-7-((trimethylsilyl)ethynyl)benzothiadiazole (TIPS-BTD-TMS)

4,7-Dibromobenzo[1,2,5]thiadiazole (1.16 g, 4 mmol) was added into a 100mL Schlenk flask filled containing a 1:1 volume/volume mixture of tetrahydrofuran (THF) and diisopropylamine (DIPA) (total volume of 16 mL). The resulting solution was then purged with argon for 30 minutes to remove any dissolved gases. Trimethylsilylacetylene (392.8 mg, 4 mmol), tri-iso-propylsilyl-acetylene (728.2 mg, 4 mmol), $Pd(PPh_3)_4$ (24 mg, 3.2 mmol), and copper iodide (8 mg, 4 mmol) was added subsequently. The solution was allowed to be stirred at room temperature for 24 hours. After this period, the solvent was removed under reduced pressure to isolate the reaction product. Flash chromatography of the residue with hexanes gave the desired product as a yellow solid. (yield 1.42 mg, 86%).

1H NMR (CDCl3, 300MHz): δ (ppm) 0.33 (s, 9H), 1.19 (s, 21H), 7.69 (m, 2H).

13C NMR (CDCl3, 300 MHz): δ (ppm) 0.09, 11.5, 18.9, 91.4, 100.3, 100.7, 102.2, 103.4, 117.1, 117.8, 132.9, 133.2, 154.4.

4-Ethynyl-7-((triisopropylsilyl)ethynyl)benzothiadiazole (TIPS-BTD)

A deoxygenated solution of TIPS-BTD-TMS (412.5 mg, 1.0 mmol) was prepared in a mixture of dichloromethane (DCM, 15 mL) and methanol (MeOH, 15 mL). Potassium carbonate (KOH, 0.17 g, 3.0 mmol) was then added to the solution under an argon atmosphere. The mixture was allowed to stir at room temperature for 1 hour. To remove any unreacted KOH, deionized water (50 mL) was added to the solution. The organic layer was then isolated and washed three times with brine and deionized water, and subsequently dried over sodium sulfate. The solvent was evaporated, leaving behind a colorless oil. The crude product was then purified via column chromatography on silica gel, using hexane as the eluent. This process resulted in a colorless liquid. The yield of the final product was 265 mg (98%).

^{1}H NMR (300 MHz, $CDCl_3$): δ (ppm) 1.18 (m, 21H), 3.66 (s, 1H) and 7.71 (m, 2H).

^{13}C NMR (75 MHz, $CDCl_3$): δ (ppm) 11.7, 19.1, 79.6, 85.2, 101.4, 102.3, 116.2, 118.7, 133.0, 133.7, 154.9.

TIPS-BTD-Pt

TIPS-BTD-MTS (63.45 mg, 0.1865 mmol) and cis-dichloro-bis-(tri-n-butylphosphine) platinum(II) (125.05 mg, 0.1875 mmol) were dissolved in diethylamine (Et_2NH, 7.5 mL). The solution was then degassed with nitrogen to ensure an oxygen-free environment. The mixture was stirred under reflux conditions for 8 hours. After that, the solvent was evaporated, leaving behind the crude product. The crude product was then purified by flash chromatography on silica gel, using hexane and then a 7:3 hexane/dichloromethane (CH_2Cl_2) mixture as eluents. This purification process resulted in the TIPS-BTD-Pt yellow solid (73 mg, 40%).

^{1}H NMR ($CDCl_3$, 300 MHz): δ (ppm) 0.88 (t, 18H), 1.19 (s, 21H), 1.41 (br m, 12H), 1.64 (br m, 12H), 2.29 (br m, 12H), 7.37 (d, 1H), 7.63 (d, 1H).

^{13}C NMR ($CDCl_3$, 75 MHz): δ (ppm) 11.5, 14.0, 18.89, 22.1, 24.5, 26.2, 97.67, 103.45, 129.5, 134, 155.

BTD-Pt

TIPS-BTD-Pt (102.2 mg, 0.105 mmol) was dissolved in THF (6.3 mL) in a 25 mL single neck round bottom flask. The solution was degassed using nitrogen and then tetrabutylammonium fluoride (60.2 mg, 0.224 mmol) was added to the reaction mixture using a syringe. This resulted in the immediate formation of a white precipitate from the initially yellow solution. The reaction was allowed to stir at room temperature for approximately 3 hours. Following this, the solvent was removed to leave behind the crude product, which was then purified by flash chromatography on silica gel. The eluents used were hexane followed by a 1:4 hexane/dichloromethane (CH_2Cl_2) mixture. This purification process yielded the desired BTD-Pt as a yellow solid. The final yield was 101.2 mg, representing a 39% yield.

^{1}NMR ($CDCl_3$, 300 MHz): δ (ppm) 0.90 (t, 18H), 1.44 (br m, 12H), 1.59 (br m, 12H), 2.09 (br m, 12H), 3.60 (s, 1H), 7.36 (d, 1H), 7.64 (d, 1H).

^{13}C NMR ($CDCl_3$, 75 MHz): δ (ppm) 14.2, 18.2, 24.2, 24.7, 26.8, 80.5, 83.4, 107.12 111.9, 124.2, 129.7, 134.6, 155.4.

p-PtBTD

BTD-Pt was dissolved in a 9mL v:v= 7:2 diisopropylamine:THF mixture in a Schlenk flask. This solution was thoroughly degassed through three successive freeze-pump-thaw cycles. The flask was then refilled with dry argon, and Tetrabutylammonium fluoride (73 mg, 0.275 mmol) was introduced via a syringe. The addition of this compound led to an immediate formation of a white precipitate from the originally yellow solution. The mixture was stirred at room temperature for approximately 40 minutes. At this point, a thin layer chromatography (TLC) analysis with 1:4 hexanes:DCM indicated complete consumption of the BTD-Pt. Copper (I) iodide (1.9 mg, 0.01 mmol) was subsequently added to the flask.

After stirring the reaction mixture overnight at room temperature, a red suspension was observed, indicative of the polymerization reaction. The reaction mixture was then poured into a nylon 66 filter (0.47μm pore size) with an excess of methanol, leading to the precipitation of the polymer as red granules. Purification procedures were three-times to obtain pure product. After the final precipitation, the polymer was dried under a vacuum at room temperature overnight to give p-PtBTD (62 mg, 65%).

^{1}H NMR (400 MHz, $CDCl_3$): δ 7.31 (br, 2H), 2.31 (br, 12H), 1.65 (br, 12H), 1.45 (br, 12H), 0.89 (br, 18H)

GPC: Mn = 15,600; Mw = 34,400, PDI= 2.20

C. NMR Spectra

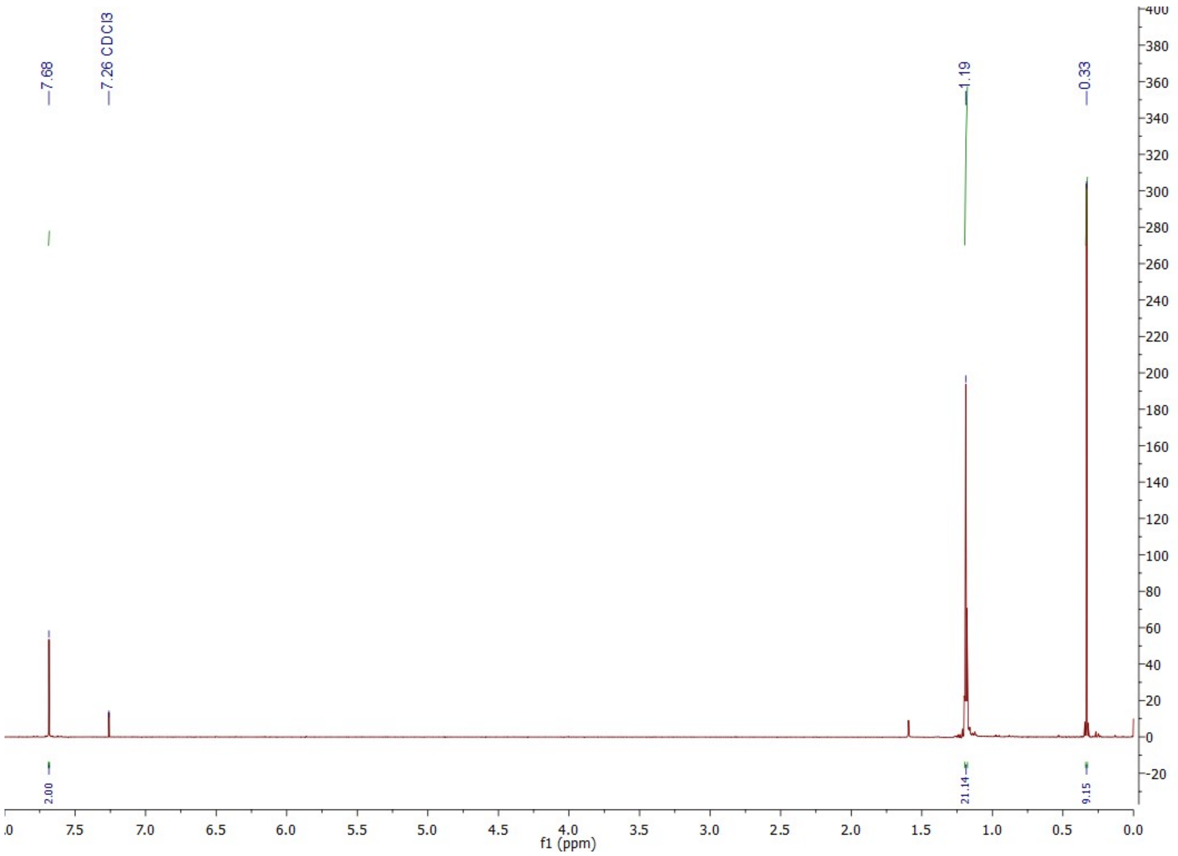

Figure S1. ^{1}H NMR spectrum of TIPS-BTD-TMS.

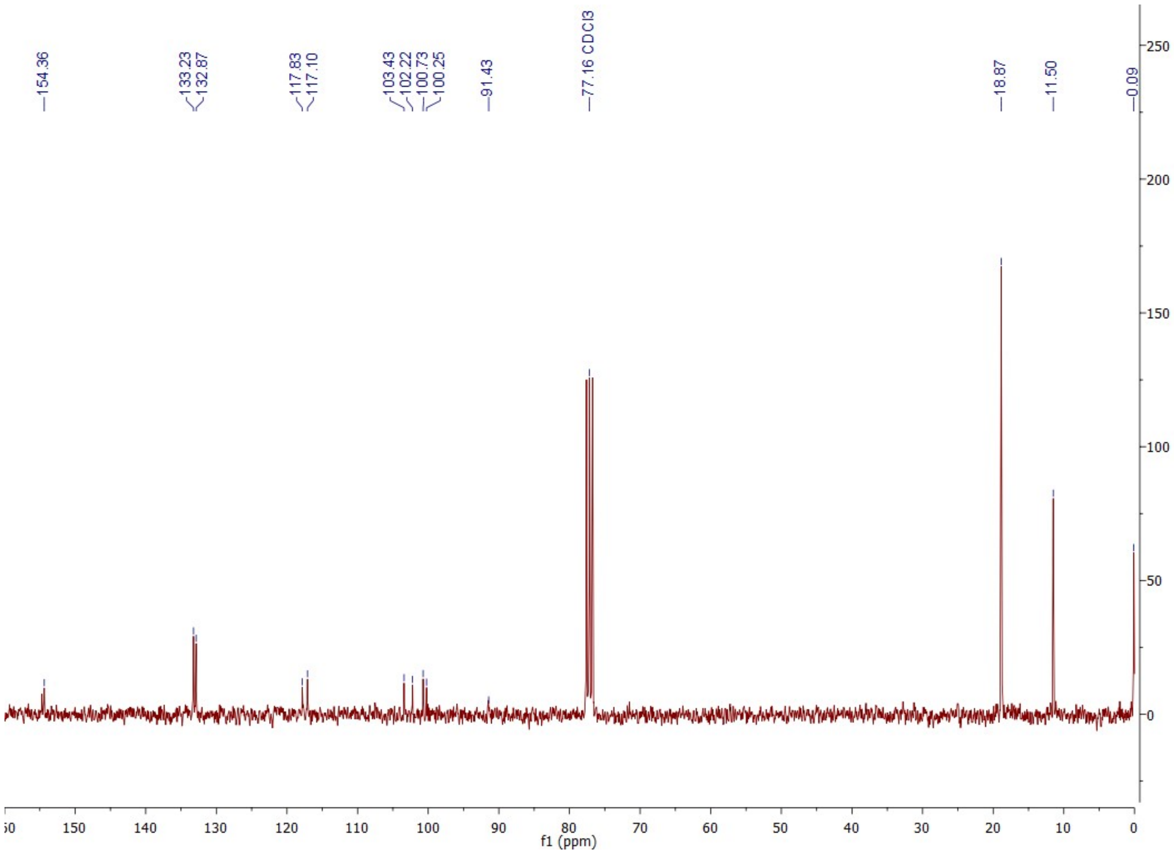

Figure S2. ^{13}C NMR spectrum of TIPS-BTD-TMS.

Figure S3. ^{1}H NMR spectrum of TIPS-BTD.

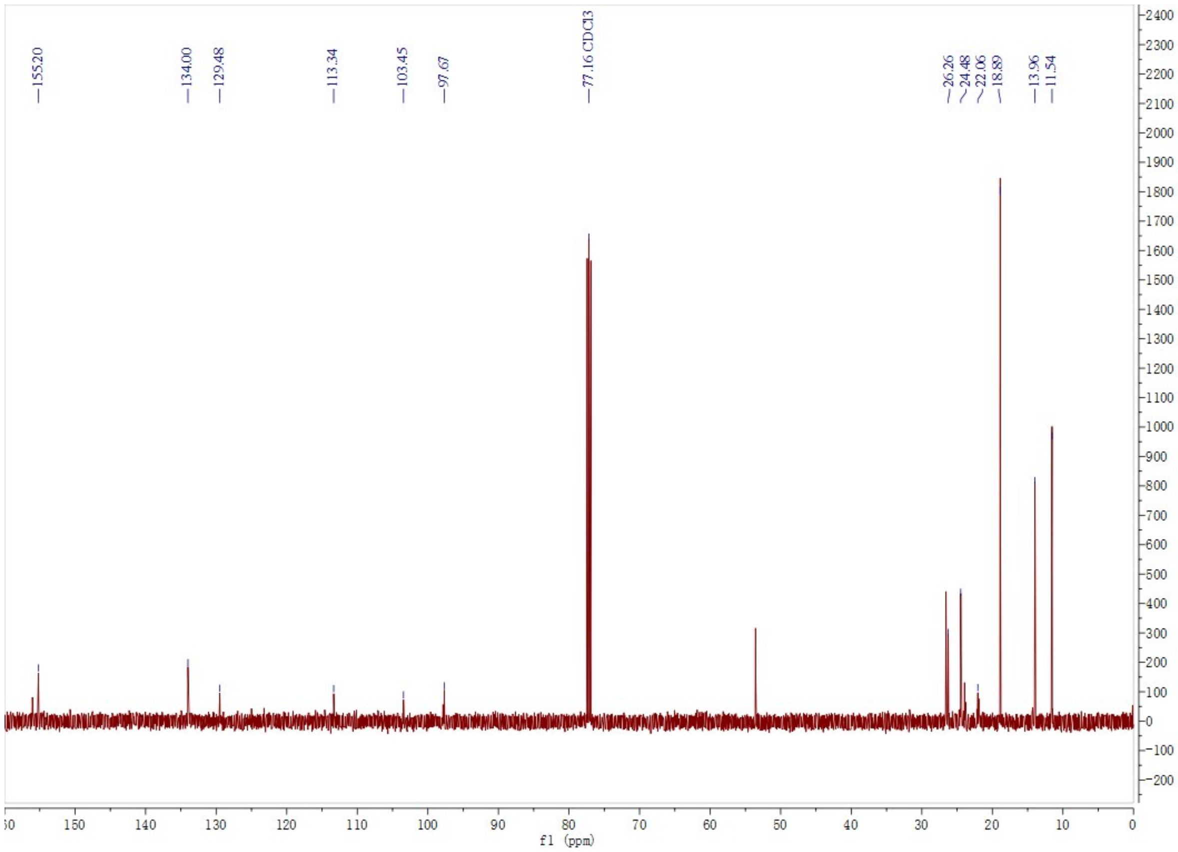

Figure S4. ^{13}C NMR spectrum of TIPS-BTD.

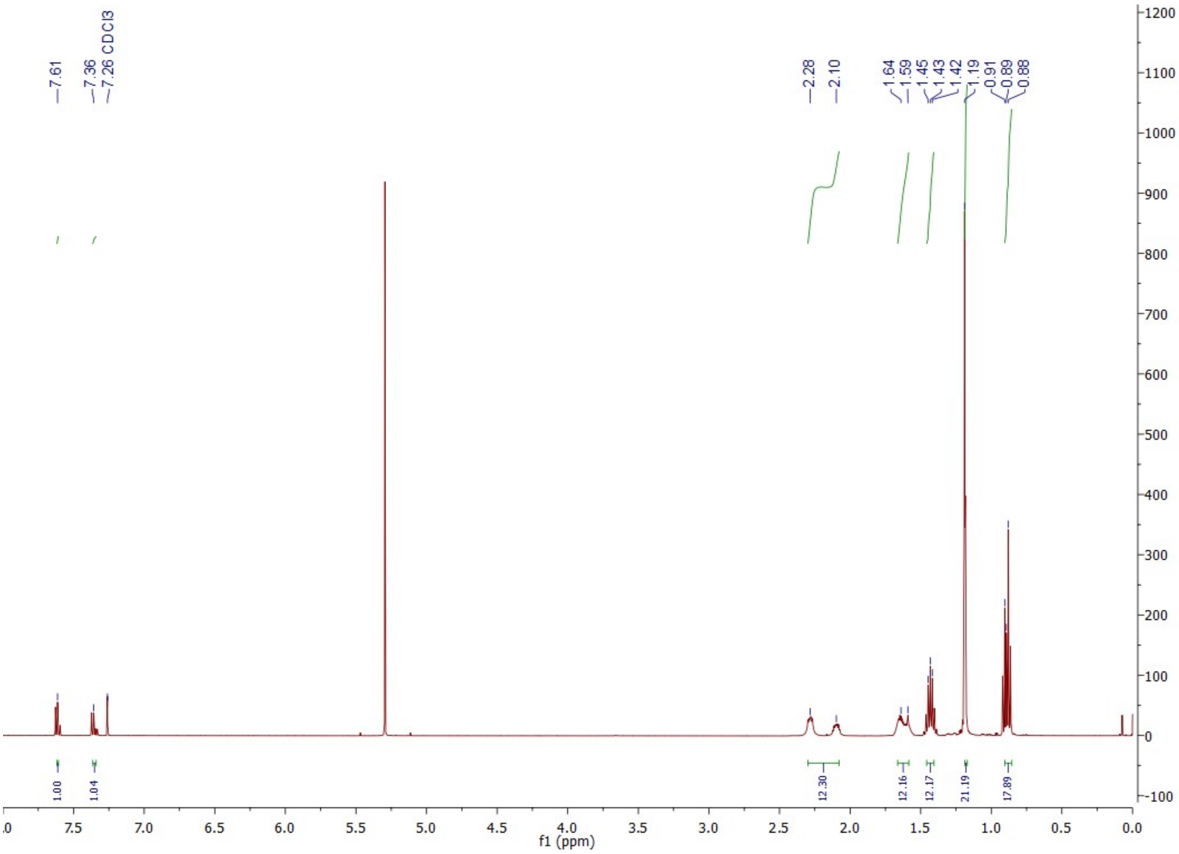

Figure S5. ^{1}H NMR spectrum of TIPS-BTD-Pt.

Figure S6. ^{13}C NMR spectrum of TIPS-BTD-Pt.

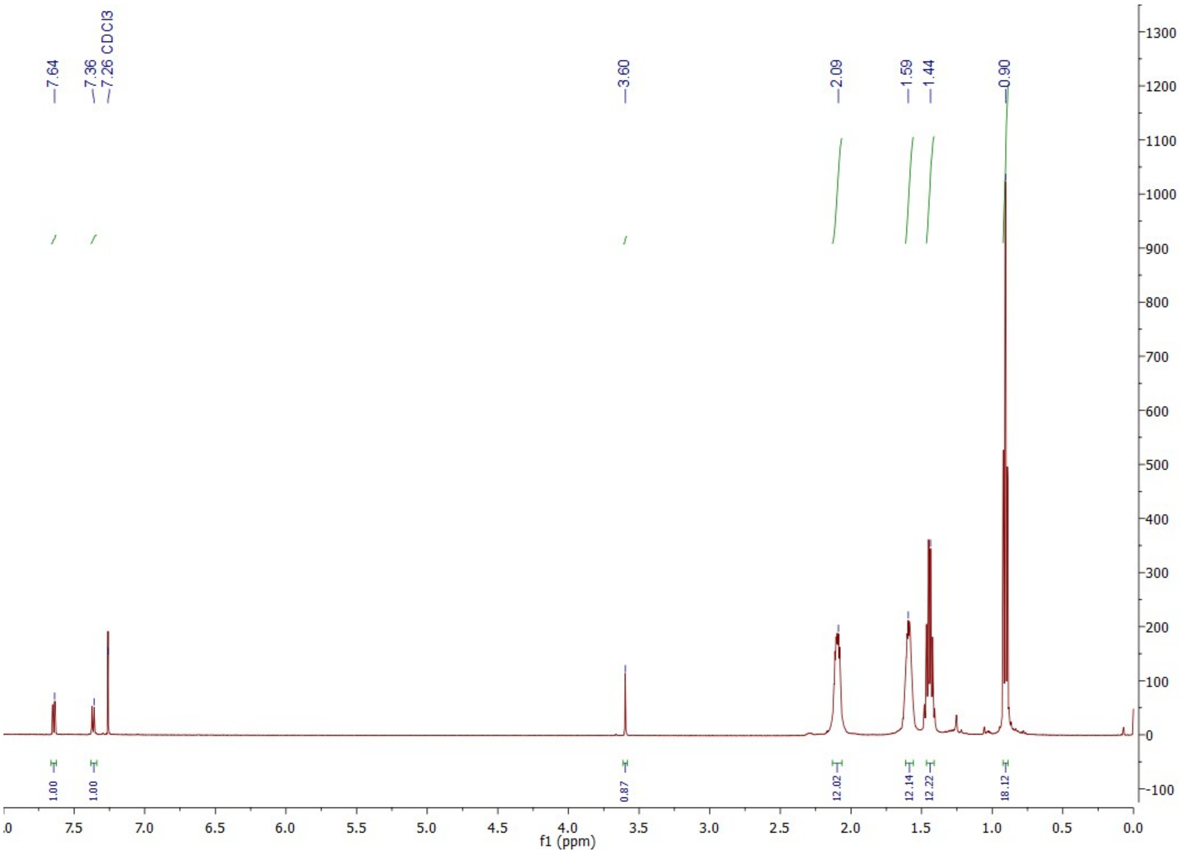

Figure S7. ^{1}H NMR spectrum of BTD-Pt.

Figure S8. ^{13}C NMR spectrum of BTD-Pt.

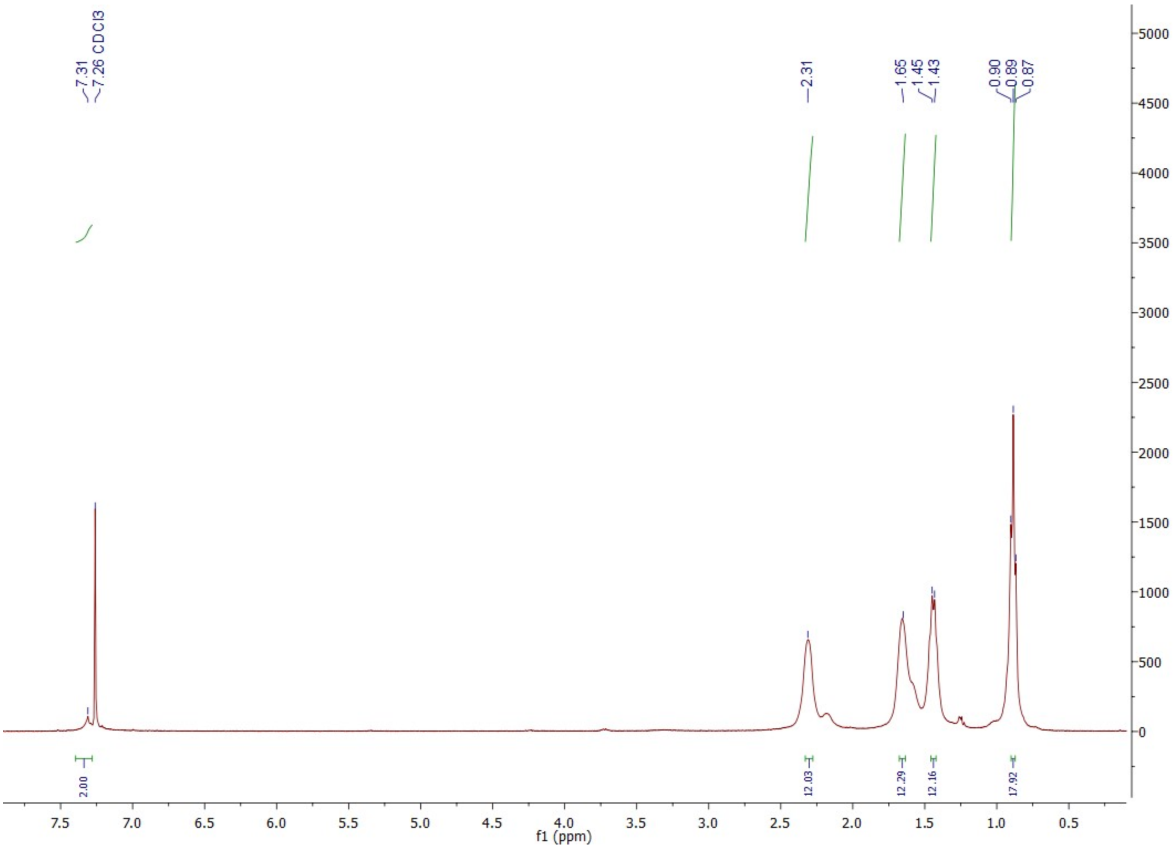

Figure S9. ^{1}H NMR spectrum of p-PtBTD.

D. Supporting Data

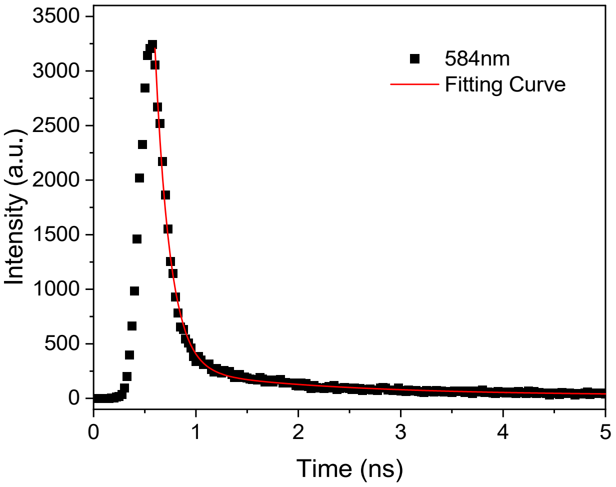

Figure S10. Transient PL decay of p-PtBTD monitored at 584 nm at 290K (back dot) and the fitting curve (red curve).

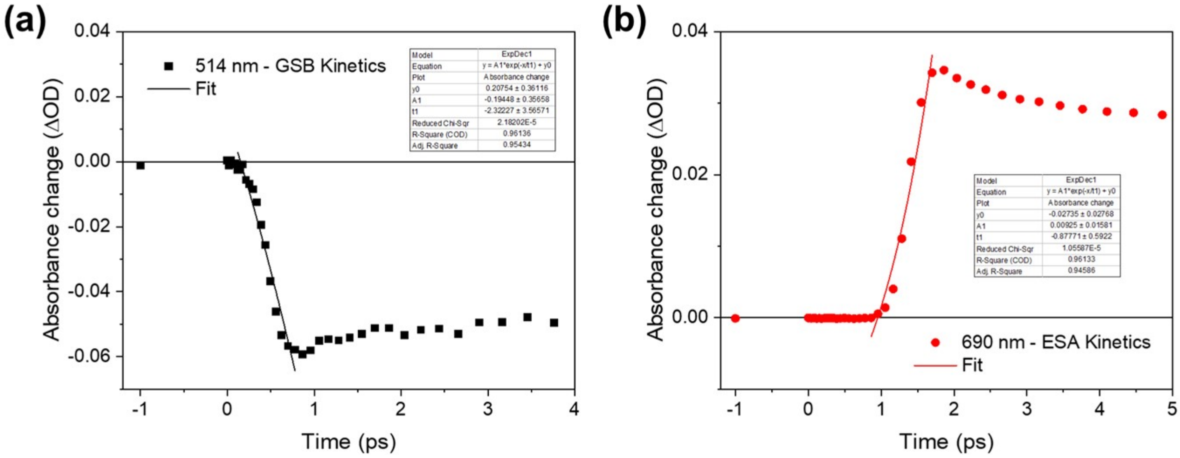

Model	ExpDec1
Equation	y = A1*exp(-x/t1) + y0
Plot	Absorbance change
y0	0.20754 ± 0.36116
A1	-0.19448 ± 0.35658
t1	-2.32227 ± 3.56571
Reduced Chi-Sqr	2.18202E-5
R-Square (COD)	0.96136
Adj. R-Square	0.95434

Model	ExpDec1
Equation	y = A1*exp(-x/t1) + y0
Plot	Absorbance change
y0	-0.02735 ± 0.02768
A1	0.00925 ± 0.01581
t1	-0.87771 ± 0.5922
Reduced Chi-Sqr	1.05587E-5
R-Square (COD)	0.96133
Adj. R-Square	0.94586

Figure S11. (a) TAS kinetic trace of p-PtBTD probed at 514 nm at 290K (back dot) and the fitting curve (black curve); **(b)** TAS kinetic trace of p-PtBTD probed at 690 nm at 290K (back dot) and the fitting curve (red curve).

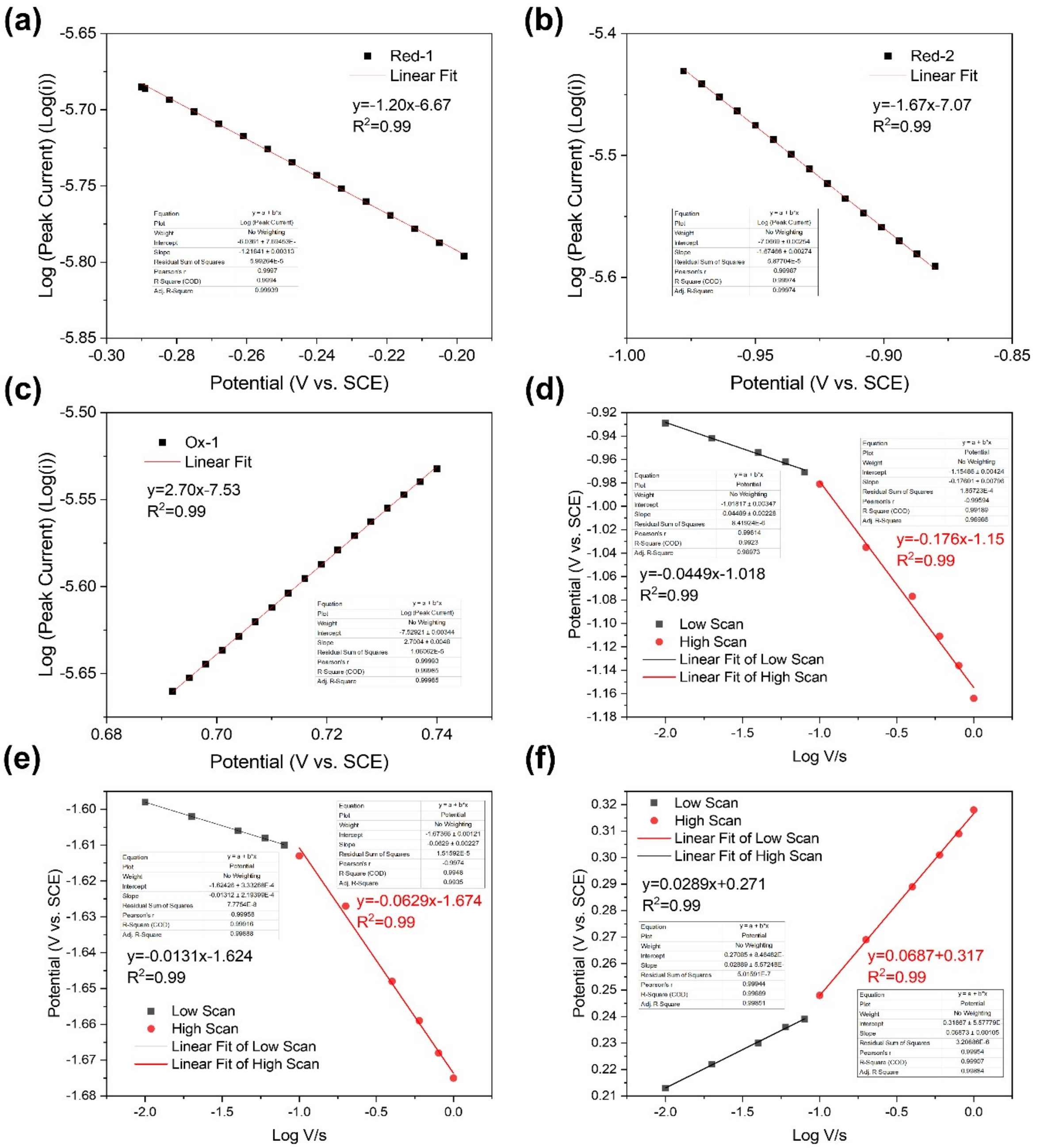

Figure S12. Tafel plot of the**(a)** 1st reduction peak, **(b)** 2nd reduction peak, and **(c)** oxidation peak of p-PtBTD; The plot of E_p against the log of scan rate at low and high scan rates of d) 1st reduction reaction, **(e)** 2nd reduction reaction and **(f)** oxidation reaction of p-PtBTD. Under the condition of 1mM p-PtBTD in 100 mM $TBAPF_6$ using DCM as solvent.

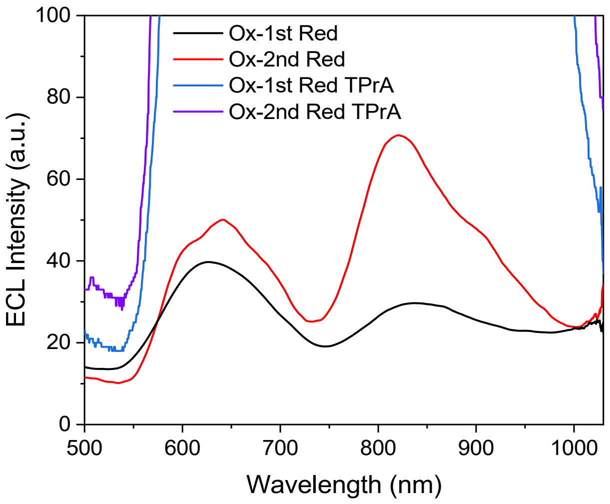

Figure S13. Enlarged ECL spectrum of 1 mM p-PtBTD pulsed in DCM between 80 mV past the reduction peak and at 80 mV past the 1st oxidation potential, respectively. Pulse width is 1 second.

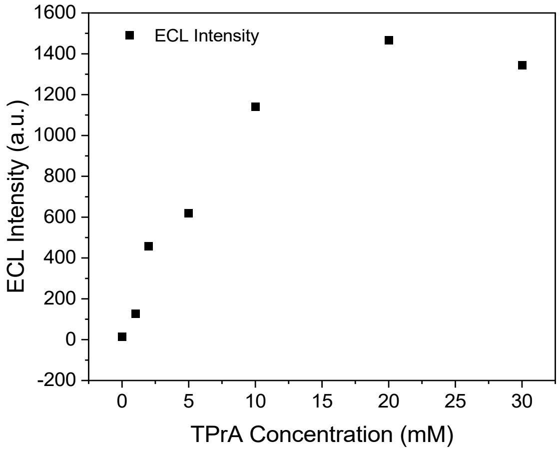

Figure S14. ECL intensity of $Rubpy_3$ and p-PtBTD under concentration of TPrA experimental conditions.

Table S1 Kinetics of p-PtBTD monitored at 584 nm at different temperatures.

Temperature (K)	**τ_1/ns (a_1)**	**τ_2/μs (a_2)**	**$< \tau_{avg} >^a$/μs**	**X^2**
340	2.0 (1.49%)	1.11 (98.51%)	1.09	0.80
310	2.3 (1.61%)	1.10 (98.39%)	1.08	0.65
280	2.5 (1.65%)	1.06 (98.35%)	1.04	0.61
250	2.9 (2.01%)	1.01 (97.99%)	0.99	0.64
220	3.4 (2.39%)	0.96 (97.61%)	0.93	0.76
190	3.8 (2.54%)	0.86 (97.46%)	0.83	0.76
160	4.2 (4.20%)	0.78 (95.84%)	0.74	0.73
130	4.3 (13.27%)	0.63 (86.73%)	0.55	0.70
100	4.3 (18.67%)	0.48 (81.67%)	0.39	0.68

[a] $\langle\tau\rangle=\sum_i \alpha_i \tau_i$

Table S2 ECL efficiencies of Rubpy$_3$ and p-PtBTD under different experimental conditions.

	ECL Efficiency (%)^b
Rubpy$_3$	**0.27**
Rubpy$_3$ with TPrA	**2.65**
p-PtBTD 1stox &1stred	**0.0020**
p-PtBTD 1stox & 2ndred	**0.0025**
p-PtBTD 1stred with TPrA	**0.12**
p-PtBTD 2ndred with TPrA	**0.18**

[b] $\phi_{ECL}=\frac{I_{ECL}}{I_{Std}}\times\phi_{Std}\times\frac{I_{E,Std}}{I_E}$ [2]

Reference

(1) Shen, M.; Rodríguez-López, J. n.; Huang, J.; Liu, Q.; Zhu, X.-H.; Bard, A. J. Electrochemistry and Electrogenerated Chemiluminescence of Dithienylbenzothiadiazole Derivative. Differential Reactivity of Donor and Acceptor Groups and Simulations of Radical Cation− Anion and Dication− Radical Anion Annihilations. *Journal of the American Chemical Society* **2010**, *132* (38), 13453-13461.

(2) Adsetts, J. R.; Chu, K.; Hesari, M.; Ma, J.; Ding, Z. Absolute electrochemiluminescence efficiency quantification strategy exemplified with Ru (bpy) 32+ in the annihilation pathway. *Analytical Chemistry* **2021**, *93* (33), 11626-11633.